ARTICLE

Semiconductor Nanowires and Nanotubes: Effects of Size and Surface-to-Volume Ratio

Hui Pan[†] and Yuan Ping Feng*

Department of Physics, National University of Singapore, 2 Science Drive 2, Singapore 117542. [†]Current address: Environmental Science Division, Oak Ridge National Laboratory, Oak Ridge, TN 37831. E-mail: panh1@ornl.gov.

ABSTRACT The electronic properties of semiconductor (SiC, GaN, BN, ZnO, ZnS, and CdS) nanowires and nanotubes were investigated using first-principles calculations based on density functional theory and generalized gradient approximation. Different size or surface-to-volume ratio dependences were found for the II—VI (ZnO, ZnS, and CdS) and IV—IV (SiC) and III—V (GaN and BN) nanostructures. For SiC, GaN, and BN nanostructures, the band gap decreases with the increase of the surface-to-volume ratio or the reduction of the diameter, while for ZnO, ZnS, and CdS nanostructures, the band gap increases with the increase of surface-to-volume ratio or the reduction of the diameter. The mechanism is attributed to the competition between the interaction from dangling *p-like* and σ states and the quantum confinement effect.

KEYWORDS: semiconductor nanowire · semiconductor nanotube · surface-to-volume ratio · size effect · first-principles calculations

One-dimension (1-D) nanostructures such as nanowires and nanotubes have been proposed as important components of electronic and optoelectronic nanodevices[1−6] and are expected to play an integral part in the design and construction of these devices. Among these nanostructures, compound semiconductor nanowires and nanotubes are attracting more and more attention due to their great potential applications in nanodevices. Experimentally, compound semiconductor nanowires/nanotubes, such as GaN, ZnO, and BN, have been synthesized using different methods.[1−6] A fundamental understanding of the 1-D semiconductor nanostructures is crucial for their applications in nanodevices. Theoretically, most works have been focused on single-walled semiconductor nanotubes such as BN, BC_2N, GaN, SiC, and AlN.[7−11] Only recently attention was paid to properties of compound nanowires. Xu *et al.* reported atomic structures and mechanical properties of realistic GaN nanotubes;[12] Wang *et al.* calculated the magnetic property of Mn-doped GaN nanowires based on first-principles,[13] and Akiyama *et al.* studied the structural stability and electronic structures of InP nanowires, also using first-principles method.[14] Recent studies on CdS, CdSe, [111] zinc-blende SiC (β-SiC), and ZnO nanowires showed that their band gaps increase with the reduction of their diameters.[15−18] However, despite these studies, the mechanism that leads to different electronic and optical properties of these nanostrucutres from the corresponding bulk materials remains unclear. There have not been many theoretical studies mainly because of the complicated structures of these 1-D nanostructures, compared to those of single-walled nanotubes. In this study, we present electronic structures of some isolated 1-D semiconductor nanostructures and investigate the size effects on the structural and electronic properties based on first-principles calculations. The results demonstrate that the size effects on the structural and electronic properties are different for different compound semiconductor 1-D nanostructures.

RESULTS AND DISCUSSION

The nanowires and nanotubes have hexagonal cross sections, which were usually observed in experiments. The initial structures were obtained from the corresponding bulk wurtzite structure. To investigate the dependence of electronic structures of the nanostructures on their size and shape, four structures of different sizes and shapes, as shown in Figure 1a, were considered for each material. For convenience, they are referred as structures n1, n2, n3, and n4 in the following discussion. Here n1, n2, and n3 are nanowires of increasing diameters, while n4 is a nanotube (hollow wire).

All structures were fully optimized. The surface passivation was not considered in our calculations as it was in literature[13,15,16,19] because these nano-

*Address correspondence to phyfyp@nus.edu.sg.

Received for review August 1, 2008 and accepted October 27, 2008.

Published online November 8, 2008. 10.1021/nn8004872 CCC: $40.75

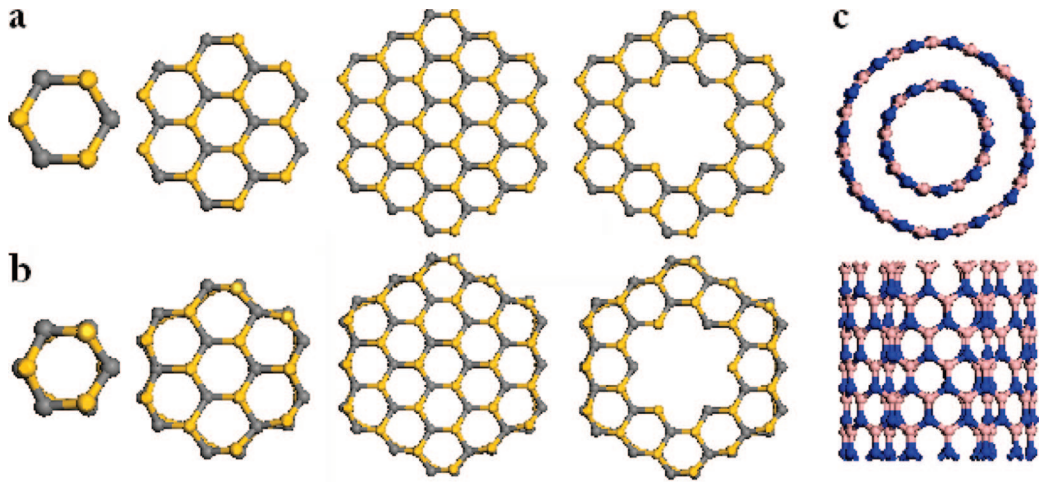

Figure 1. Top view of atomic configuration of wurtzite nanostructures (n1−n4) before (a) and after (b) optimization and the geometry of BN nanotube (BN−n4) after optimization (c).

structures were often synthesized at high temperature. For SiC, GaN, ZnO, ZnS, and CdS nanostructures, there were no significant changes in the structures after the geometry optimization (Figure 1b), except relaxation of some surface atoms. Most of the surface atoms were found to relax inward, but the degrees of relaxation are different for different atoms. For example, the inward relaxation of the surface Si atoms is much more significant than that of C atoms for the SiC nanowire. The surface atom relaxation leads to about 5% contraction of the bond along the [0001] direction and approximately 2% contraction in other surface bonds. The relaxation also results in deviations of the bonding angles from the tetrahedral bonding angle in bulk semiconductors. For example, the C−Si−C and Si−C−Si angles in the relaxed SiC−n2 became 114.8 and 104.2°, respectively. Similarly, geometric optimization resulted in little changes in the structures of the BN nanowires (n1−n3). However, the structure of the BN nanotube (BN−n4) changed significantly after geometric optimization. BN−n4 (Figure 1c) became a double-walled nanotube after the geometric optimization, similar to that observed in experiments.[20] It consists of an inner zigzag single-walled BN nanotube (SWBNNT) (9,0) and an outer SWBNNT (15,0). The interwall distance is about 2.89 Å, which is similar to the reported distance.[21] The formation of a double-walled BN nanotube is attributed to the stable sp^2 hybridization, which is lower in energy than sp^3 hybridization for BN, and the formation of the π states leads to destruction of the sp^3 hybridization and the formation of the double-walled nanotube. The results of our calculation indicate that single-walled BN nanotubes are stable, which had been produced experimentally.[22]

Figure 2 shows the band structures of the SiC 1-D nanostructures. The smallest nanowire (SiC−n1) is metallic due to contribution of the π bonding (Figure 2a) which leads to the top valence energy level and bottom conduction energy level crossing the Fermi level. The larger SiC nanowires exhibit an indirect band gap which is similar to that of bulk w-SiC (Figure 2b,c2). The valence band top is located at Γ point and the conduction band bottom at ~2/3 along ΓZ. The band gaps are 1.63 and 1.66 eV for SiC−n2 and SiC−n3 within GGA, respectively, which are smaller than the calculated value of bulk w-SiC.[23] Figure 2d shows the band structure of the SiC nanotube (SiC−n4). The indirect band gap is 0.87 eV with the valence band top at Γ and the conduction band bottom at Z. Electron density analysis indicates that the top valence band of the SiC nanowires consists of the p-like dangling bonds of surface carbon atoms and σ bonding states of interior carbon atoms (Figure 3a,b), and the bottom conduction band is ascribed to the p-like dangling bonds at the surface of the nanowire (Figure 3c,d). The interaction among these states is responsible for the dispersion of the lowest conduction band and the highest valence band (Figure 2). It is noted that the band gap decreases with the increase of the surface-to-volume ratio (Table 2), and the band gap of the SiC nanotube is much smaller than those of nanowires. The reason could be the interaction between the p-like orbitals

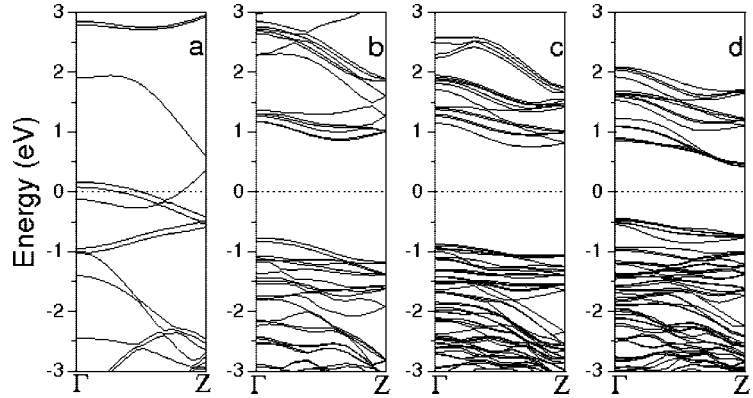

Figure 2. Calculated band structures for SiC nanostructures (a) SiC−n1, (b) SiC−n2, (c) SiC−n3, and (d) SiC−n4.

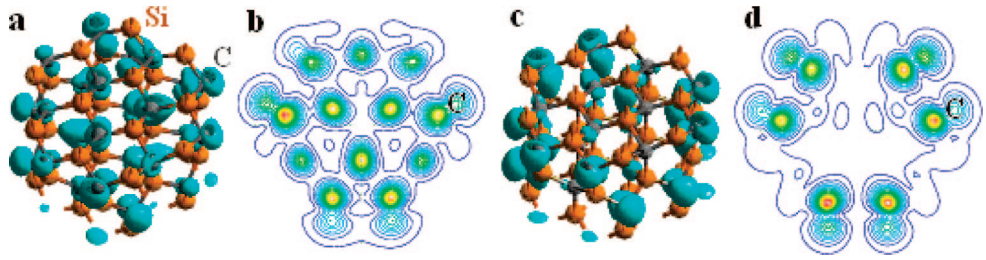

Figure 3. Calculated electron densities for (a) SiC−n2 valence top, (b) the contour presentation of the valence top, (c) SiC−n2 conduction bottom, and (d) the contour presentation of the conduction bottom.

and σ states which shifts the σ and p bands to lower and higher energies, respectively, and the effect is more apparent in the SiC−n4. The repulsion between σ and p states leads to the reduction of band gap in small nanowires. It should be noticed that our results on [0001] wurtzite SiC nanostructure contrast that on [111] hydrogen-saturated β-SiC nanowires.[18] The reason is attributed to the surface states and coupling between the p-like orbitals and σ states in our SiC systems, while the quantum confinement effect was dominant in [111] β-SiC nanowires due to hydrogen termination on the surface.[18] The Si and C atoms in the SiC nanowires and nanotubes are sp^3-hybirdized, resulting in a dangling sp^3 bond on each surface atom. These dangling sp^3 bonds are responsible for the surface states of the SiC nanostructures. The surface states are removed from the band gap of SiC nanostructures, when the sp^3 bonds are passivated by hydrogen atom. Therefore, the band gap of hygrogenated SiC nanowires decreases with the increase of wire radius due to the quantum confinement effect.

All GaN 1-D nanostructures considered in the study exhibit a direct band gap which increases with the reduction of the surface-to-volume ratio or the increase of the diameter (Table 1). The calculated band gaps are 1.26 eV for GaN−n1, 1.61 eV for GaN−n2, 1.81 eV for GaN−n3, and 1.73 eV for GaN−n4 within GGA. Similar to SiC 1-D nanostructures, this can be attributed to the interaction between the p-like orbitals and σ states.

The smallest BN nanowire (BN−n1) has a direct band gap of 1.33 eV at Γ point, which is consistent with that of small radius BN nanotubes.[24] The band structures of larger BN nanowires (BN−n2 and BN−n3) show indirect band gap, similar to bulk w-BN. The valence band top is located at Γ point and the conduction band bottom at 3/5 along ΓZ. The band gap increases from 3.96 eV for BN−n2 to 4.06 eV for BN−n3 with the reduction of the surface-to-volume ratio. Not like SiC−n4, BN−n4 becomes a double-walled nanotube after geometric optimization. It can be expected that its electronic properties are similar to those of multiwalled BN nanotubes (MWBNNTs).[21] BN−n4 is a direct band semiconductor with a band gap of 2.68 eV, which is smaller than those of the inner SWBNNT (9,0) (3.62 eV) and outer SWBNNT (15,0) (4.31 eV).[24] The possible reason is the hybridization between the π and σ state of each tube. The valence band top is the π-like state of the outer tube, whereas the conduction band bottom is the π* state of the inner tube. The hybridization induces shifts of the bands and leads to the reduction of the band gap in MWBNNTs.[24] For other BN nanostructures (BN−n2 and BN−n3), the band gap increases with the reduction of the surface-to-volume ratio are due to the interaction between the p-like orbitals and σ states, which is similar to the situation of the SiC 1-D nanostructure.

Band structures shown in Figure 4 indicate that ZnO nanostructures retain the direct band gap property of bulk w-ZnO. The calculated band gaps are 2.09 eV for ZnO−n1, 1.56 eV for ZnO−n2, and 1.17 eV for ZnO−n3 within GGA (Table 1), while that of ZnO nanotube (ZnO−n4) is 1.47 eV (Figure 4). Our calculations show that the band gap increases with the increase of the surface-to-volume ratio or the reduction of the diameter (Table 2), which is consistent with the theoretical and experimental result.[19,25] Electron density analysis indicates that p-like dangling bond states of O atoms at the surface of the nanowires mainly contribute to the top valence band in ZnO 1-D nanostructures (Figure 5a,b). These p-like states interact with each other, resulting in the dispersion of the corresponding energy level as shown in Figure 4. Similar situations were ob-

TABLE 1. Calculated Band Gaps of the Wurtzite Semiconductor and Their Corresponding Nanostructures

	bulk (eV)	n1 (eV)	n2 (eV)	n3 (eV)	n4 (eV)
SiC	2.41(*id*)	metallic	1.63(*id*)	1.66(*id*)	0.87(*id*)
GaN	1.94(*d*)	1.26(*d*)	1.61(*d*)	1.81(*d*)	1.73(*d*)
BN	5.73(*id*)	1.33(*d*)	3.96(*id*)	4.06(*id*)	2.68(*d*)
ZnO	0.82(*d*)	2.09(*d*)	1.56(*d*)	1.17(*d*)	1.47(*d*)
ZnS	2.14(*d*)	2.80(*d*)	2.76(*d*)	2.46(*d*)	2.57(*d*)
CdS	1.34(*d*)	2.42(*d*)	1.95(*d*)	1.49(*d*)	1.72(*d*)

TABLE 2. Value of Surface-to-Volume Ratio of the Semiconductor Nanostructures

	n1	n2	n3	n4
SiC	—	0.434	0.260	0.651
GaN	—	0.418	0.251	0.627
BN	—	0.526	0.315	0.789
ZnO	—	0.410	0.246	0.626
ZnS	—	0.350	0.210	0.525
CdS	—	0.322	0.193	0.483

tained for ZnS and CdS nanostructures, where the increase of the surface-to-volume ratio or the reduction of the diameter leads to an increase of the band gap (Table 1). For CdS nanostructures, our results are consistent with those in ref 15. The trend of band gap with the surface-to-volume ratio or diameter in ZnO, ZnS, and CdS is opposite to that in SiC, GaN, and BN 1-D nanostructures but similar to Si[26] and ZnSe nanowires.[27] The quantum confinement theory is accepted for the band gap expansion of a nanometric semiconductor. The confinement effect on the band gap (E_G) of a nanosolid is expressed as a function of particle size (R):[28]

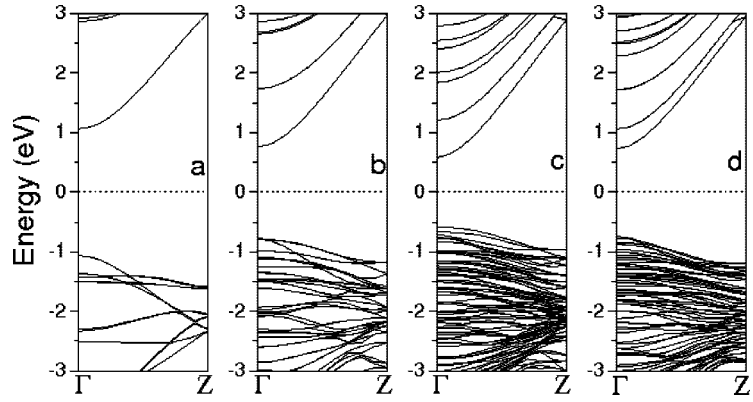

Figure 4. Calculated band structures for ZnO nanostructures (a) ZnO−n1, (b) ZnO−n2, (c) ZnO−n3, and (d) ZnO−n4.

$$E_G(R) = E_G(\text{bulk}) + \frac{2h^2}{2\mu R^2} - \frac{1.786e^2}{\varepsilon_r R} + 0.284E_R \quad (1)$$

where μ and ϵ_r are the effective dielectric constant and effective mass, respectively, which describe the effect of the homogeneous medium in the quantum box. E_R is the Rydberg (spatial correlation) energy for bulk semiconductor.

According to the quantum confinement theory, electrons in the conduction band and holes in the valence band are confined spatially by the potential barrier of the surface or trapped by a monopotential well of the quantum box. Because of the confinement of both electrons and holes, the optical transition energy from the valence top to the conduction bottom increases. From the electron density analysis (Figure 5), the interaction between the p-like orbitals and σ states cannot be observed from the electron density analysis. These p-like states result in the separation of the energy levels, which is responsible for the quantum confinement effect. Therefore, the possible mechanism for the expansion of the band gap in II−VI nanostructures is attributed to the quantum confinement effect, which results in the increase of band gap with the increase of the surface-to-volume ratio or the reduction of the diameter, because the interaction between the p orbitals and σ states effect can be neglected in these II−VI nanostructures.

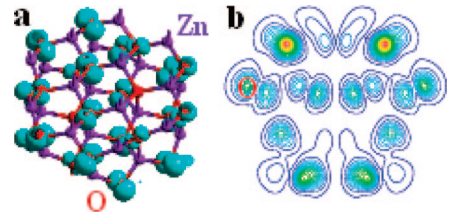

Figure 5. Calculated electron densities for (a) ZnO−n2 valence top and (b) the contour presentation of the valence top.

CONCLUSION

In summary, the effects of size and surface-to-volume ratio on the electronic properties of wurtzite semiconductor nanowires and nanotubes were investigated by first-principles method. The calculations demonstrated that only for BN−n4 can the double-walled BN nanotube be formed after geometry optimization, indicating that single-walled BN nanotubes are easier to be produced experimentally than other semiconductor single-walled nanotubes. The trend of band gap with the size or surface-to-volume ratio is attributed to the interaction between the p-like orbitals and σ states or quantum confinement effect. For SiC, GaN, and BN nanostructures, the interaction between the p-like orbitals and σ states is dominant, which leads to the decrease of the band gap with the increase of the surface-to-volume ratio or the reduction of the diameter. For ZnO, ZnS, and CdS nanostructures, the quantum confinement effect is dominant and results in the increase of the band gap with the increase of the surface-to-volume ratio or the reduction of the diameter. Although the well-known fact that DFT/GGA underestimates the band gap of semiconductors, the dependence of the electronic properties of semiconductor nanostructures on their size and surface-to-volume ratio is valid.

METHODS

First-principles method based on the density functional theory (DFT)[29] and the generalized gradient approximation (GGA)[30] are used to investigate the structural and electronic properties of 1-D semiconductor nanostructures. In our study, we used the plane-wave basis DFT pseudopotential method and the CASTEP code.[31] The ionic potentials were described by ultrasoft pseudopotentials proposed by Vanderbilt.[32] The completely filled semicore Zn and Cd 3d electrons are treated the same as the other valence states. The Monkhorst and Pack scheme of k point sampling was used for integration over the first Brillouin zone.[33] An energy cutoff of 400 eV and 10 k points along the axis of the tube in the reciprocal space were used in our calculation. Good convergence was obtained with these parameters, and the

total energy was converged to 2.0×10^{-5} eV/atom. A large supercell dimension with a wall-to-wall distance of 10 Å in the plane perpendicular to the tube axis was used to avoid interaction between the 1-D nanostructure and its images in neighboring cells. The unit is periodic in the direction of the nanotube/nanowire axis along the [0001] of the wurtzite semiconductor.

REFERENCES AND NOTES

1. Javey, A.; Guo, J.; Farmer, D.;B.; Wang, Q.; Yenilmez, E.; Gordon, R. G.; Lundstrom, M.; Dai, H. J. Self-Aligned Ballistic Molecular Transistors and Electrically Parallel Nanotube Arrays. *Nano Lett.* **2004**, *4*, 1319–1322.
2. Tseng, G. S.; Ellenbogen, J. C. Toward Nanocomputers. *Science* **2001**, *294*, 1293–1294.
3. Huang, Y.; Duan, X.; Cui, Y.; Lieber, C. M. Gallium Nitride Nanowire Nanodevices. *Nano Lett.* **2002**, *2*, 101–104.
4. Duan, X.; Huang, Y.; Cui, Y.; Wang, J.; Lieber, C. M. Indium Phosphide Nanowires as Bblocks for Nanoscale Electronic and Optoelectronic Devices. *Nature* **2001**, *409*, 66–69.
5. Wang, Z. L. Zinc Oxide Nanostructures: Growth, Properties and Applications. *J. Phys.: Condens. Matter* **2004**, *16*, R829–R858.
6. Barrelet, C. J.; Greytak, A. B.; Lieber, C. M. Nanowire Photonic Circuit Elements. *Nano Lett.* **2004**, *4*, 1981–1985.
7. Rubio, A.; Corkill, J. L.; Cohen, M. L. Theory of Graphitic Boron Nitride Nanotubes. *Phys. Rev. B* **1994**, *49*, 5081–5084.
8. Pan, H.; Feng, Y. P.; Lin, Y. *Ab Initio* Study of Single-Wall BC_2N Nanotubes. *Phys. Rev. B* **2006**, *74*, 045409-1–045409-4.
9. Lee, S. M.; Lee, Y. H.; Hwang, Y. G.; Elsner, J.; Frauenheim, T. Stability and Electronic Structure of GaN Nanotubes from Density-Functional Calculations. *Phys. Rev. B* **1999**, *60*, 7788–7791.
10. Zhao, M.; Xia, Y.; Zhang, D.; Mei, L. Stability and Electronic Structure of AlN Nanotubes. *Phys. Rev. B* **2003**, *68*, 235415-1–235415-4.
11. Menon, M.; Richter, E.; Mavrandonakis, A.; roudakis, G.; Andriotis, A. N. Structure and Stability of SiC Nanotubes. *Phys. Rev. B* **2004**, *69*, 115322-1–115322-4.
12. Xu, B.; Lu, A. J.; Pan, B. C.; Yu, Q. X. Atomic Structures and Mechanical Properties of Single-Crystal GaN Nanotubes. *Phys. Rev. B* **2005**, *71*, 125434-1–125434-6.
13. Wang, Q.; Sun, Q.; Jena, P. Ferromagnetism in Mn-Doped GaN Nanowires. *Phys. Rev. Lett.* **2005**, *95*, 167202-1–167202-4.
14. Akiyama, T.; Nakamura, K.; Ito, T. Structural Stability and Electronic Structures of InP Nanowires: Role of Surface Dangling Bonds on Nanowire Facets. *Phys. Rev. B* **2006**, *73*, 235308-1–235308-6.
15. Huang, S. P.; Cheng, W. D.; Wu, D. S.; Hu, J. M.; Shen, J.; Xie, Z.; Zhang, H.; Gong, Y. J. Density Functional Theoretical Determinations of Electronic and Optical Properties of Nanowires and Bulks for CdS and CdSe. *Appl. Phys. Lett.* **2007**, *90*, 031904-1–031904-3.
16. Fan, W.; Xu, H.; Rosa, A. L.; Frauenheim, Th.; Zhang, R. Q. First-Principles Calculations of Reconstructed [0001] ZnO Nanowires. *Phys. Rev. B* **2007**, *76*, 073302-1–073302-4.
17. Xu, H.; Rosa, A. L.; Frauenheim, Th.; Zhang, R. Q.; Lee, S. z. Density-Functional Theory Calculations of Bare and Passivated Triangular-Shaped ZnO Nanowires. *Appl. Phys. Lett.* **2007**, *91*, 031914-1–031914-3.
18. Yan, B.; Zhou, G.; Duan, W.; Wu, J.; Gu, B. L. Uniaxial-Stress Effects on Electronic Properties of Silicon Carbide Nanowires. *Appl. Phys. Lett.* **2006**, *89*, 023104-1–023104-3.
19. Xiang, H. J.; Yang, J.; Hou, J. G.; Zhu, Q. Piezoelectricity in ZnO Nanowires: A First-Principles Study. *Appl. Phys. Lett.* **2006**, *89*, 223111-1–223111-3.
20. Fuentes, G. G.; Borowiak-Palen, E.; Pichler, T.; Liu, X.; Graff, A.; Behr, G.; Kalenczuk, R. J.; Knupfer, M.; Fink, J. Electronic Structure of Multiwall Boron Nitride Nanotubes. *Phys. Rev. B* **2003**, *67*, 035429-1–035429-6.
21. Okadaa, S.; Saito, S.; Oshiyama, A. Electronic and Geometric Structures of Multi-Walled BN Nanotubes. *Physica B* **2002**, *323*, 224–226.
22. Bengu, E.; Marks, L. D. Single-Walled BN Nanostructures. *Phys. Rev. Lett.* **2001**, *86*, 2385–2387.
23. Xu, Y. N.; Ching, W. Y. Electronic, Optical, and Structural Properties of Some Wurtzite Crystals. *Phys. Rev. B* **1993**, *48*, 4335–4351.
24. Xiang, H. J.; Yang, J.; Hou, J. G.; Zhu, Q. First-Principles Study of Small-Radius Single-Walled BN Nanotubes. *Phys. Rev. B* **2003**, *68*, 035427-1–035427-5.
25. Gu, Y.; Kuskovsky, I. L.; Yin, M.; O'Brien, S.; Neumark, G. F. Quantum Confinement in ZnO Nanorods. *Appl. Phys. Lett.* **2004**, *85*, 3833–3835.
26. Zhao, X.; Wei, C. M.; Yang, L.; Chou, M. Y. Quantum Confinement and Electronic Properties of Silicon Nanowires. *Phys. Rev. Lett.* **2004**, *92*, 236805-1–035427-4.
27. Xia, J. B.; Cheah, K. W. *Phys. Rev. B* **1997**, *55*, 15688–15693.
28. Kayanuma, Y. Quantum-Size Effects of Interacting Electrons and Holes in Semiconductor Microcrystals with Spherical Shape. *Phys. Rev. B* **1988**, *38*, 9797–9805.
29. Hohenberg, P.; Kohn, W. Inhomogeneous Electron Gas. *Phys. Rev.* **1964**, *136*, B864–B871.
30. Perdew, J. P.; Wang, Y. Accurate and Simple Analytic Representation of the Electron-Gas Correlation Energy. *Phys. Rev. B* **1992**, *45*, 13244–13249.
31. Payne, M. C.; Teter, M. P.; Allan, D. C.; Arias, T. A.; Joannopoulos, J. D. Iterative Minimization Techniques for *Ab Initio* Total-Energy Calculations: Molecular Dynamics and Conjugate Gradients. *Rev. Mod. Phys.* **1992**, *64*, 1045–1097.
32. Vanderbilt, D. Soft Self-Consistent Pseudopotentials in a Generalized Eigenvalue Formalism. *Phys. Rev. B* **1990**, *41*, 7892–7895.
33. Monkhorst, H. J.; Pack, J. Special Points for Brillouin-Zone Integrations. *Phys. Rev. B* **1976**, *13*, 5188–5192.